Drug Development and Industrial Pharmacy, 2010; 36(8): 980–992

informa
healthcare

ORIGINAL ARTICLE

Thermal stability and nonisothermal kinetics of Folnak® degradation process

Bojan Janković and Slavko Mentus

Faculty of Physical Chemistry, Department for Dynamics and Matter Structure, University of Belgrade, Belgrade, Serbia

Abstract

Aim: The purpose of this article is to investigate the thermal stability and nonisothermal kinetics of Folnak® drug degradation process using different thermoanalytical techniques. *Methods*: The nonisothermal degradation of Folnak® powder samples was investigated by simultaneous thermogravimetry–differential thermal analysis, in the temperature range from ambient to 810°C. *Results*: It was found that the degradation proceeds through five reaction stages, which include the dehydration, the melting process of excipients, the decomposition of folic acid, corn starch, and saccharose. The presence of compounds such as excipients increases the thermal stability of the drug and some kind of solid–solid and/or solid–gas interaction occurs. *Conclusion*: It was concluded that the main degradation stage of Folnak® sample represents the decomposition of folic acid. It was established that the folic acid decomposition cannot be explained by simple reaction order model ($n = 1$) but with the complex reaction mechanism that includes higher reaction orders ($n > 1$). The isothermal predictions of the folic acid decomposition at four different temperatures (T_{iso} = 180°C, 200°C, 220°C, and 260°C) were established. It was concluded that the shapes of conversion curves at lower temperatures (180–200°C) were similar, whereas they became more complex with further temperature increase because of the complexity of the decomposition reaction.

Key words: *Drug interactions; excipients; kinetics; nonlinear regression; stability; thermogravimetric analysis*

Introduction

Folic acid, *N*-[*ρ*-[[(2-amino-4-hydroxy-6-pteridinyl) methyl]-amino]benzoyl]-L-glutamic acid, is a B-complex vitamin containing a pteridine moiety linked by a methylene bridge to *p*-aminobenzoic acid, which is joined by a peptide linkage to glutamic acid. Conjugates of folic acid are present in a wide variety of foods, particularly liver, kidneys, yeast, and leafy green vegetables[1].

Commercially available folic acid is prepared synthetically. Folic acid occurs as a yellow or yellowish-orange crystalline powder and is very slightly soluble in water and insoluble in alcohol. Folic acid is readily soluble in dilute solutions of alkali hydroxides and carbonates, and solutions of the drug may be prepared with the aid of sodium hydroxide or sodium carbonate, thereby forming the soluble sodium salt of folic acid (sodium folate). Aqueous solutions of folic acid are heat-sensitive and rapidly decompose in the presence of light and/or riboflavin[2–4].

From the clinical pharmacology point of view, folic acid acts on megaloblastic bone marrow to produce a normoblastic marrow. In man, an exogenous source folate is required for the synthesis of nucleoprotein and the maintenance of normal erythropoiesis[5,6]. Folic acid is the precursor of tetrahydrofolic acid, which is involved as a cofactor for transformylation reactions in the biosynthesis of purines and thymidylates of nucleic acids[7]. Impairment of thymidylate synthesis in patients with folic acid deficiency is thought to account for the defective DNA synthesis that leads to megaloblast formation and megaloblastic and macrocytic anemias.

Folic acid is effective in the treatment of megaloblastic anemias because of a deficiency of folic acid (as may be seen in tropical or nontropical sprue)[8,9] and in anemias of nutritional origin, pregnancy, infancy, or childhood.

Address for correspondence: Dr. Bojan Janković, Faculty of Physical Chemistry, Department for Dynamics and Matter Structure, University of Belgrade, Studentski trg 12–16, PO Box 137 , Belgrade 11001, Serbia. Tel/Fax: ++381-11-2187-133. E-mail: bojanjan@ffh.bg.ac.rs

(Received 23 Sep 2009; accepted 16 Jan 2010)

ISSN 0363-9045 print/ISSN 1520-5762 online © Informa UK, Ltd.
DOI: 10.3109/03639041003628890

Thermal analysis is a term used to describe the analytical techniques that measure the physical and the chemical properties of a sample as a function of temperature or time[10]. The importance of thermal analysis methods has been emphasized by Waterman and Adami[11] in their review of methods of rapidly and accurately assessing the chemical stability of pharmaceutical dosage forms[12]. Thermal analysis is a routine method for the analysis of drugs and substances of pharmaceutical interest[13].

Thermogravimetry (TG), in which the change in mass of a sample heated at constant rate is recorded and plotted versus temperature, is an effective method of studying thermal stability and for determining the kinetic parameters of the decomposition of drugs and medicines[14,15]. It can be used in the quality control of drugs, with a view to improve the final product and to determine drug quality through technological parameters[16]. In TG, the substance mass as a function of time and temperature is used to assess the thermal stability and degradation of drugs, which include the generation of kinetic data such as the apparent activation energies.

In the solid state, the temperatures required for thermal degradation at a measurable rate are generally far higher than the temperatures existing, even locally, during photolysis[17]; so the mechanisms of thermal and photochemical degradation can be expected to differ. On the contrary, it is well known that at high temperatures the chemical reactivity of drug active components, both pure and in the mixture, can be modified, thus leading to uncontrollable reactions with consequent dangerous situations. For this reason, it is important to determine the thermal stability (i.e., the temperature range over which a substance does not degrade with an appreciable rate).

This work aims to study the thermal stability and the kinetic behavior of nonisothermal degradation process of Folnak® (Folic Acid), the commercial drug product manufactured by Sigmapharm D.O.O. company (Niš, Serbia).

In this article, thermogravimetric analysis (TGA), differential thermogravimetry (DTG), and differential thermal analysis (DTA) data from Folnak® samples have been investigated and the global kinetic analysis has been carried out. Basically, TGA, DTG, and DTA data have been used for the estimation of the effective kinetic parameters of the investigated process.

Materials and methods

Materials

The one-wrapping Folnak® tablets were supplied by Sigmapharm D.O.O. company. The tablet of ardently yellow color was crushed to a powdery form before they were used in thermoanalytical measurements.

In the Folnak® tablet, the active pharmaceutical ingredient represents the folic acid. The excipients in the investigated Folnak® tablets are the following: corn starch, saccharose, stearic acid, and polyethylene glycol 4000 (PEG-4000). The mentioned excipients, except the stearic acid, belong to the binders. The stearic acid belongs to the lubricants.

Methods

Thermoanalytical measurements

The SDT 2960, simultaneous TG–DTA thermobalance manufactured by TA Instruments (New Castle, DE, USA), was used to examine the nonisothermal degradation of Folnak® samples.

The device calibration was performed as recommended by the manufacturer. TGA weight calibration was based on two temperature runs, between room temperature and 1000°C: one using empty balance beams and the other using beams charged by the standard alumina calibrating weights. The temperature calibration was performed by means of phase transitions of KNO_3 (128°C), $KClO_4$ (300°C), K_2SO_4 (583°C), and melting point of NaCl (801°C) in Pt 110 mL pans, used for the Folnak® analysis, too.

The Folnak® powder samples were heated at the rates of β = 2.5°C/min, 5°C/min, 10°C/min, and 20°C/min, and the flow rate of the purging gas (Nitrogen—N_2) was 100 mL/min. The samples were heated in the temperature range from ambient to 810°C. The loading amount was 2.0 ± 0.1 mg. After cooling to room temperature, a black residue was observed in the sample pan, which was assumed to be carbon.

To confirm the repeatability and the authenticity of the generated data for all considered cases, the experiments were repeated three times at every heating rate and the average TG trace among them was used as the representative thermoanalytical curve. The observed deviations were very small.

Kinetic procedure

Kinetic analysis of a degradation process is traditionally expected to produce an adequate kinetic description of the process in terms of the reaction model and the Arrhenius parameters using a single-step kinetic equation[18]:

$$\frac{\mathrm{d}\alpha}{\mathrm{d}t} = k(T)f(\alpha), \tag{1}$$

where t is the time, T the temperature, α the extent of conversion, and $f(\alpha)$ the reaction model. The temperature

dependence of the rate constant is introduced by replacing $k(T)$ with Arrhenius equation, which gives Equation (2) as follows:

$$\frac{\mathrm{d}\alpha}{\mathrm{d}t} = A\exp\left(-\frac{E_a}{RT}\right)f(\alpha), \tag{2}$$

where A (the pre-exponential factor) and E_a (the apparent activation energy) are the Arrhenius parameters and R is the gas constant. For the nonisothermal conditions, $\mathrm{d}\alpha/\mathrm{d}t$ in Equation (2) is replaced with $\beta(\mathrm{d}\alpha/\mathrm{d}T)$, where β is the linear heating rate, giving

$$\frac{\mathrm{d}\alpha}{\mathrm{d}T} = \frac{A}{\beta}\exp\left(-\frac{E_a}{RT}\right)f(\alpha). \tag{3}$$

Integration of Equation (3), after replacing E_a/RT by x and rearranging, leads to

$$\int_0^{\alpha}\frac{\mathrm{d}\alpha}{f(\alpha)} = g(\alpha) = \frac{AE_a}{\beta R}p(x), \tag{4}$$

where $g(\alpha)$ is the function of the reaction model in the integral form, $p(x)$ ($x = E_a/RT$) is a function known as the Arrhenius integral that has no analytical solution but can be resolved either by numerical methods or by using different approximations. In this article, we used the Senum and Yang fourth rational approximation for $p(x)$ function[19].

The extent of conversion, α (fraction of compound decomposed), in nonisothermal conditions can be presented as $\alpha(T) = (\%m_i - \%m_T)/(\%m_i - \%m_f)$, where $\%m_i$ is the initial percent mass, $\%m_T$ the percent mass at temperature T, and $\%m_f$ the final percent mass, as they are collected from a nonisothermal TG experiment. The three components [A, E_a, and $f(\alpha)$] called 'kinetic triplet' define both in Equations (2) and (3) a single-step reaction that disagrees with the multistep nature of decomposition that usually occurs in the solid state. As the studied compounds have complex structures, it can be hypothesized that several steps with different energies will be involved.

If a process involves several steps with different apparent activation energies, the relative contributions of these steps to the overall reaction rate will vary with both temperature and the extent of conversion. This means that the effective activation energy determined from the analysis of the results will also be a function of these two variables.

Following the model-fitting method[20], the $k(T)$ term is determined by the form of the $f(\alpha)$ chosen. The evaluation of the $f(\alpha)$ term is achieved by fitting various reaction models to experimental data. A single nonisothermal experiment provides information on both $k(T)$ and $f(\alpha)$ terms but not in a separate form. For this reason, almost any $f(\alpha)$ can satisfactorily fit experimental data by virtue of the variation in the Arrhenius parameters that compensate the difference between the assumed model for $f(\alpha)$ and the true but unknown one[21].

The complex nature of a multistep process can be more easily detected when using a broader temperature range in the nonisothermal conditions. An alternative approach to kinetic analysis are the model-free methods[20,22] that allow us for evaluating E_a without choosing the reaction model. The isoconversional methods[22] make up the best representation of the model-free approach. These methods yield the variation of the effective activation energy as a function of the extent of conversion[20,21]. Hence, constant E_a values can be expected in the case of single-step process, whereas in a multistep process E_a varies with α due to the variation in the relative contributions of each single step to the overall reaction rate.

Isoconversional (model-free) methods

These methods are known to allow for model-independent estimates of the apparent activation energy. Their use allows the investigation of the dependence of the apparent activation energy on conversion degree. In this work, the two integral isoconversional methods [Kissinger–Akahira–Sunose (KAS)[23,24] and Ozawa[25] methods] were used. Using differential isoconversional method (such as the Friedman method[26]) is avoided because this method is very sensitive in the case when the experimental curve is fluctuating[27]. On the contrary, the differential isoconversional method has a strong weakness: experimental noise is magnified, which renders the whole task of evaluating the values of the apparent activation energy very difficult, sometimes even impossible. In integral isoconversional methods, results are less affected by experimental errors and these methods are based on the primary experimentally acquired data, α and T.

As we indicated above, because this procedure may lead to erroneous estimates of the apparent activation energy, the use of the integral isoconversional methods appears to be a safer alternative.

Kissinger–Akahira–Sunose method

KAS[23,24] method is the isoconversional integral method based on the Coats–Redfern[28] approximation of the Arrhenius integral. It was shown that

$$\ln\left(\frac{\beta}{T^2}\right) = \ln\left[\frac{AR}{E_a g(\alpha)}\right] - \frac{E_a}{RT}. \tag{5}$$

Thus, for α = constant, the plot $\ln(\beta/T^2)$ versus $1/T$, obtained from curves recorded at several heating rates, should be a straight line whose slope can be used to evaluate the apparent activation energy.

Ozawa method

If we use the Doyle's approximation[29] for $p(x)$, we get from Equation (4) the popular equation proposed by Ozawa[25] for determining the apparent activation energy by isoconversional methods:

$$\ln\beta = \ln\left[\frac{AE_a}{Rg(\alpha)}\right] - 5.330 - 1.052\frac{E_a}{RT}. \quad (6)$$

Equation (6) shows that, provided that $g(\alpha)$ is constant at a given value of α, the slope of the plots of $\ln\beta$ versus $1/T$ for particular values of α leads to the apparent activation energy as a function of α independent of the kinetic model fitted by the reaction.

Determination of the kinetic model

Once the apparent activation energy has been determined, we can find the kinetic model that best describes a measured set of thermoanalytical data. Málek[30] has shown that for this purpose it is useful to define two special functions $y(\alpha)$ and $z(\alpha)$, which can easily be obtained by simple transformation of experimental data.

Through the rearrangement of Equation (2), the function $y(\alpha)$ is defined as[31] follows:

$$y(\alpha) = \frac{d\alpha}{dt}\exp\left(\frac{E_a}{RT}\right) = Af(\alpha). \quad (7)$$

The $y(\alpha)$ function is proportional to the $f(\alpha)$ function. Thus by plotting $y(\alpha)$ dependence, normalized within (0,1) interval, the shape of function $f(\alpha)$ is obtained. The $y(\alpha)$ function is, therefore, characteristic for a given kinetic model $f(\alpha)$ and it can be used as a diagnostic tool for the kinetic model determination. The characters of the $y(\alpha)$ function with respect to various kinetic model functions are reported previously[30]. It should be stressed that the shape of the $y(\alpha)$ function is strongly affected by E_a value. Hence the true apparent activation energy is decisive for a reliable determination of the kinetic model because of the correlation of the kinetic parameters[30].

If the temperature rises at a constant rate β, integration of Equation (2) gives the following equation:

$$g(\alpha) = \int_0^\alpha \frac{d\alpha}{f(\alpha)} = \frac{AE_a}{\beta R}\exp(-x)\left[\frac{\pi(x)}{x}\right]. \quad (8)$$

By combining Equations (2) and (8), an alternative kinetic equation is obtained:

$$\frac{d\alpha}{dt} = \left[\frac{\beta}{T\pi(x)}\right]f(\alpha)g(\alpha). \quad (9)$$

After rearrangement of Equation (9), the $z(\alpha)$ function is defined as follows[32]:

$$z(\alpha) = \pi(x)\frac{d\alpha}{dt}\frac{T}{\beta} = f(\alpha)g(\alpha), \quad (10)$$

where $\pi(x)$ is the temperature integral. In this article, the fourth-degree Senum and Yang formula[19] was used for $\pi(x)$.

The shape of the $y(\alpha)$ function as well as the maximum α_p^∞ of the $z(\alpha)$ function can be used as a guide to select the kinetic model. Both α_m (the maximum of the $y(\alpha)$ function) and α_p^∞ parameters are especially useful in this respect. Their combination allows the determination of the most suitable kinetic model[30].

Because the $y(\alpha)$ and $z(\alpha)$ functions are invariable with respect to temperature or the heating rate, being quite sensitive to subtle changes in the kinetic model $[f(\alpha)]$, they can be conveniently used as the suitable tools for kinetic model determination.

Prediction of isothermal degradation process

Prediction of isothermal degradation process from nonisothermal runs is of scientific and practical interest. First, good prediction of isothermal degradation process from parameters obtained during nonisothermal degradation clearly validates the reaction model. Second, the isothermal degradation characterization is notoriously challenging from the experimental standpoint.

Kinetic computations can be used for drawing mechanistic conclusions or for making simulations of the process. One of the most used simulation is called 'isothermal predictions'[20], which means that the nonisothermal kinetic parameters can be used to simulate the variation of the extent of conversion (α) versus time (t) for a given (constant) temperature (T_{iso}). Isoconversional methods are very powerful for this task because they allow these simulations to be made without any assumption on the reaction mechanism and without evaluation of the pre-exponential factor (A). These simulations can be obtained using the following equation[20]:

$$t_\alpha = \left[\beta\exp\left(-\frac{E_{a,\alpha}}{RT_{iso}}\right)\right]^{-1}\sum_0^\alpha \int_{T_\alpha-\Delta\alpha}^{T_\alpha}\exp\left(-\frac{E_{a,\alpha}}{RT}\right)dT, \quad (11)$$

where t_α is the time to reach a given conversion (α), β is the heating rate of the nonisothermal experiment used

for the computation, and T_{iso} is the isothermal temperature of the isothermal simulation. In Equation (11), the integral was evaluated by the numerical integration of the data, and the extent of conversion (α) was varied between α = 0.05 and α = 0.95. As can be seen from Equation (11), these simulations can be done using the sole $E_{a,\alpha}$—dependence computed with the KAS isoconversional method.

Results and discussion

TG–DTG–DTA curves of Folnak® degradation

Figures 1 and 2 show the mass loss (TG) and differential mass loss (DTG) curves in relation to the heating rate to a final temperature of 810°C for the Folnak® samples. All Folnak® samples exhibit same patterns of thermal degradation as the temperature is increased. The analysis of these curves demonstrates that there are five stages of mass loss profile (Figure 1), best illustrated in the derivative curves (Figure 2).

The lower temperature region, from ambient up to approximate 110°C, produces mass loss that has been attributed to the polymer dehydration[33–36]. The excipients as corn starch and the PEG-4000 (Figure 3) all exhibited a broad endothermic effect in the temperature range of 30–110°C because of the loss of water molecules. This reaction stage is designated as I on corresponding TG and DTG curves at all heating rates (Figures 1 and 2).

The DTA curve of the Folnak® degradation process at heating rate of 10°C/min (Figure 3) shows a single sharp endothermic peak, which can be attributed to the excipients (in the first place for PEG-4000 and stearic acid) melting, typical of crystalline anhydrous substances. This reaction stage (in the temperature range of 110–170°C) is designated as II on corresponding TG and DTG curves at all heating rates (Figures 1 and 2). It should be noted that the melting temperature depends on the water content and lies above 100°C at a low moisture content (such as for pure corn starch)[37].

It can be pointed out that impure materials generally have lower melting points and exhibit less well-defined peaks in thermograms. In the absence of an interaction, this effect is usually negligible. For the nonisothermal degradation of Folnak® samples we have a opposite case, for which it can be concluded that solid–solid interaction probably exists[14,38]. It can be pointed out that a noticeable upward shift of peak temperature by more than 60°C was observed.

The region of mass loss from about 170°C to 280°C is because of the folic acid in Folnak® degradation process. Namely, the main mass loss begins at about 170°C, which represents the starting point for the folic acid degradation. The mass loss in this stage is about 26% of the total mass loss (Table 1). This reaction stage is

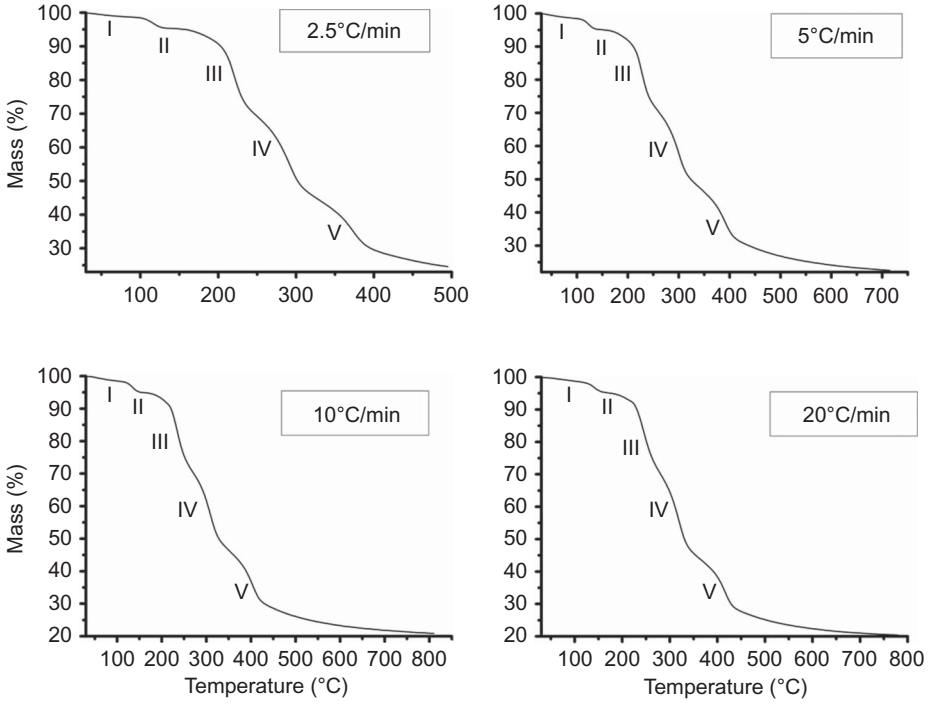

Figure 1. TG curves [mass (%) versus T (°C)] of the nonisothermal degradation of the Folnak® samples recorded in nitrogen atmosphere at heating rates of 2.5°C/min, 5°C/min, 10°C/min, and 20°C/min (the corresponding degradation stages are designated as stages I, II, III, IV, and V).

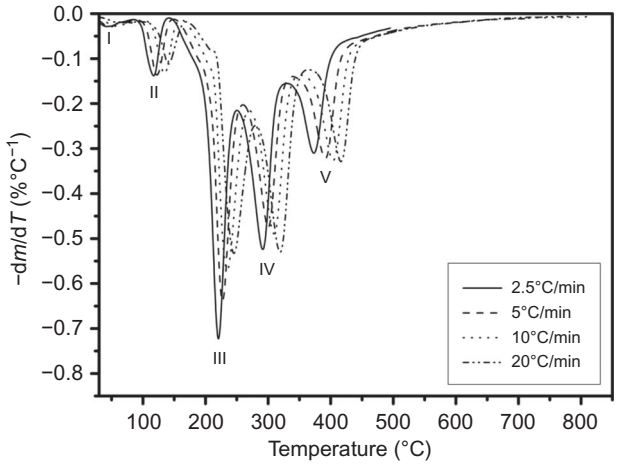

Figure 2. DTG curves [−dm/dT (%/°C) versus T(°C)] of the nonisothermal degradation of the Folnak® samples recorded in nitrogen atmosphere at heating rates of 2.5°C/min, 5°C/min, 10°C/min, and 20°C/min (the corresponding degradation stages are designated as stage I, II, III, IV, and V).

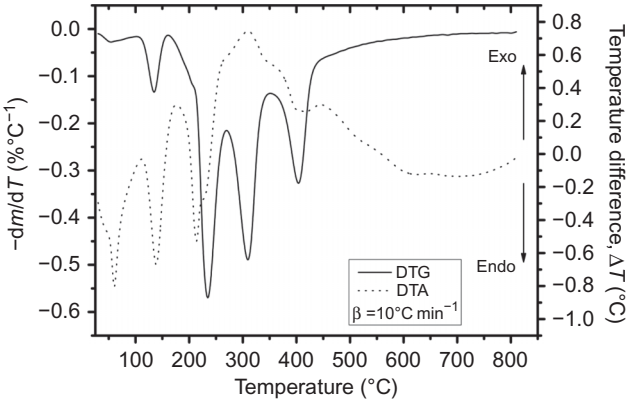

Figure 3. The simultaneous recorded DTA–DTG curve at a heating rate of β = 10°C/min, for the nonisothermal degradation process of the Folnak® sample.

designated as III on corresponding TG and DTG curves at all heating rates (Figures 1 and 2).

Table 1 shows the values of characteristic temperatures and corresponding mass losses attached with every observed reaction stages for the investigated Folnak® degradation process.

It can be seen from Table 1 that with increase in heating rate (β), the values of characteristic temperatures (T_i—initial (onset), T_m—maximum, and T_f—final temperatures; T_i represents the temperature at which the process starts and T_f represents the temperature at which the process ends) also increase, which is typical for thermally activated processes. The temperatures T_i and T_f were determined using the extrapolation method of data processing[39–41]. Table 1 shows that there was a lateral shift to higher temperatures (T_m) as the heating rate was increased. The lateral shift has been assigned as being due to the combined effects of the heat transfer at the different heating rates and the kinetics of the degradation resulting in delayed degradation.

It can be observed from Figure 3 (DTA curve at 10°C/min) that the folic acid does not have an observed melting temperature in the investigated Folnak® sample. In the case of Folnak® nonisothermal degradation, the third reaction stage probably proceeds through the apparent melting and degradation of folic acid, which is manifested by the highly endothermic peak with appearance of right shoulder at approximately 225°C in the DTA (Figure 3). It can be concluded that the third DTG peak and the highly endothermic peak in the DTA were attributed to the loss of the glutamic acid moiety[42]. This moiety begins to degrade at around 170°C. The DTA results showed an endothermic peak at 215°C, which was because of the initial melting followed by the degradation.

In the fourth stage, between 280°C and 365°C, the mass loss is attributed to the decomposition of corn starch[33]. It can be seen that relatively large exothermic peak at 310°C in the DTA curve (Figure 3) mainly can be attributed to the decomposition of amylopectin. This reaction stage is designated as IV on corresponding TG and DTG curves at all heating rates (Figures 1 and 2).

Table 1. Values of characteristic temperatures (T_i, T_m, and T_f) and mass losses (Δm) Corresponding to five stages of the nonisothermal degradation process of Folnak® sample.

	Stage I				Stage II				Stage III				Stage IV				Stage V			
β (°C/min)	T_i[a] (°C)	T_m[b] (°C)	T_f[c] (°C)	Δm_I (%)	T_i[a] (°C)	T_m[b] (°C)	T_f[c] (°C)	Δm_{II} (%)	T_i[a] (°C)	T_m[b] (°C)	T_f[c] (°C)	Δm_{III} (%)	T_i[a] (°C)	T_m[b] (°C)	T_f[c] (°C)	Δm_{IV} (%)	T_i[a] (°C)	T_m[b] (°C)	T_f[c] (°C)	Δm_V (%)
2.5	30	40	90	1.26	90	120	145	3.42	145	220	250	26.04	250	290	330	24.87	330	375	495	19.76
5	30	45	95	1.39	95	125	150	3.46	150	225	260	24.66	260	300	345	23.54	345	395	715	24.38
10	30	55	105	1.54	105	135	160	3.49	160	235	270	24.53	270	310	355	23.59	355	405	740	24.81
20	30	65	110	1.36	110	140	170	3.41	170	245	280	24.94	280	320	365	23.52	365	415	775	23.29

[a]T_i, the initial (onset) temperature.
[b]T_m, the temperature at maximum degradation rate.
[c]T_f, the final temperature.

In the fifth stage, for the temperature range from 365°C to approximately 800°C, the thermal decomposition of saccharose (sucrose) has occurred[43], with endothermic peak at about 400°C on the corresponding DTA curve for the heating rate of 10°C/min (Figure 3). The considered reaction stage is designated as V on corresponding TG and DTG curves at all heating rates (Figures 1 and 2). At the same time, the presence of CO_2 (which evolved as a product of carbonate decomposition) at high temperature reacted with residual char to form CO also causing some mass loss (these mass losses occur after the following temperatures: T = 395°C, 420°C, 435°C, and 445°C at 2.5°C/min, 5°C/min, 10°C/min, and 20°C/min, respectively) (Figure 1). This additional mass loss is included in the fifth degradation stage of investigated Folnak® sample (Table 1). At the end of the considered TG measurements, the carbon residue has occurred as the final product.

To eliminate the influence of heating rates on the nonisothermal degradation process of Folnak® samples, T_m was taken as an example to quantitatively investigate the difference between the degradation steps that include the different reaction components. As shown in Figure 4, T_m of Folnak® sample increased linearly along with the heating rates (β). The relationship between T_m and β can be expressed in the following equation:

$$T_m = T_m^0 + A^*\beta, \tag{12}$$

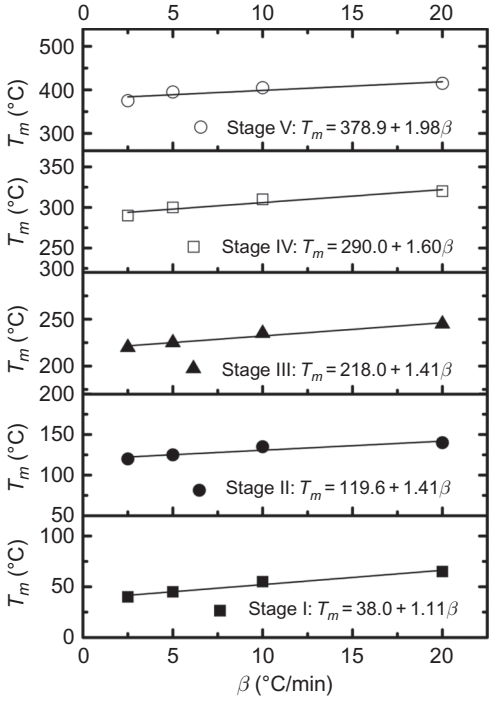

Figure 4. The plots of T_m versus heating rates of the Folnak® samples for all considered degradation stages. The functional relationships between T_m and β for the investigated system are given in the same figure.

where T_m^0 is the equilibrium temperature of the maximum degradation rate, at the heating rate assumed to be equal to 0°C/min and A^* is the rate constant.

The T_m^0 of Folnak® sample increased from 38.0°C (for the first degradation stage) to 378.9°C (for the fifth degradation stage) with $\Delta T_m^0 = 340.9$°C (Figure 4), which probably indicates the presence of solid–solid and/or solid–gas interactions. For detail investigation of excipient interactions, some of the spectroscopic experimental techniques can be applied (e.g., the NMR spectroscopy)[44]. The A^* value increases from 1.1 (first degradation stage) to 2.0 (fifth degradation stage) (Figure 4), which indicates that the fifth degradation stage of Folnak® sample has more improved thermal transport barrier effect than the first degradation stage.

Determination of kinetic parameters

The kinetics of thermal degradation reactions of carbonaceous materials is complex; in that degradation of carbonaceous materials involves a large number of reactions in parallel and in series. To determine the kinetic parameters for the third degradation stage, we take out 19 'α' values from the investigated samples at the different heating rate and read the corresponding temperature from the original conversion-temperature data.

According to Equations (5) and (6), the apparent activation energy can be evaluated from the slope of these linear relationships. The obtained results from the applied KAS and Ozawa isoconversional methods suggest that the correlation of the regression lines is very good and the magnitude of correlation coefficient exceeds 0.99, which shows that both isoconversional methods are appropriate. Figure 5 illustrates the variations of the apparent activation energy (E_a) with the extent of conversion (α) evaluated by using the KAS and

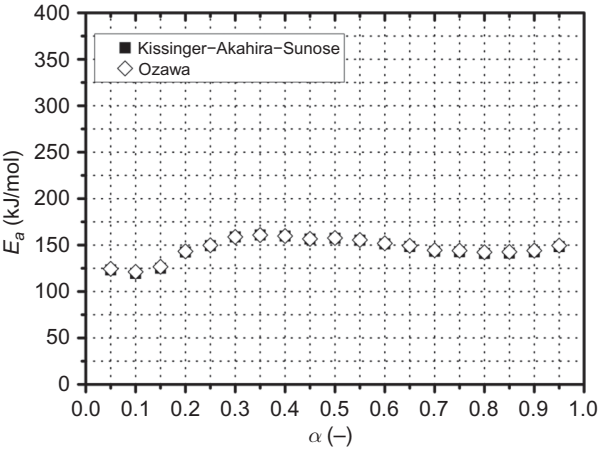

Figure 5. Dependence of E_a on α calculated by the Kissinger–Akahira–Sunose (KAS) and Ozawa isoconversional (model-free) methods for the third degradation stage of the Folnak® sample.

Ozawa model-free methods, for the third degradation stage of Folnak® sample.

From Figure 5 we can conclude that the apparent activation energy of the considered third degradation stage of Folnak® sample (stage which includes the folic acid decomposition as the active substance in the Folnak® sample) is not a definite value throughout the reaction process, which shows that the third degradation stage is a complex multistep reaction and in the different temperature ranges the degradation reaction has the different apparent activation energies and reaction mechanisms. However, it can be observed that there is no significant variation of the apparent activation energy values with the extent of conversion in the range of [0.30, 0.80]. Both isoconversional methods provide a check of invariance of E_a with respect to α in the range of [0.30, 0.80], which is one of the basic assumptions in kinetic analysis of thermoanalytical data. These results indicate that the activation energy of the third degradation stage of Folnak® sample in the considered α range changed slightly and the average values of E_a calculated by KAS and Ozawa model-free methods are as follows: $<E_a>_{KAS}$ = 152.3 kJ/mol and $<E_a>_{Ozawa}$ = 152.8 kJ/mol. It can be observed that excellent agreement exists between these two values of E_a calculated by the KAS and Ozawa methods.

Complex processes are characterized by the dependences of E_a and A and α. This generally reflects the existence of a compensation effect through the equation evaluated by the KAS method:

$$\ln\left[\frac{A_\alpha}{g(\alpha)}\right] = -12.41252 + 0.28438E_{a,\alpha}, \qquad (13)$$

where a = −12.41252 minutes^{-1} and b = 0.28438 mol/kJ are the compensation effect parameters. This equation represents an isokinetic relationship (IKR) and can be deduced by the reordering of the equation that describes the kinetics of the reaction. It is established that only one mechanism is present when an IKR exists. The slope $b = 1/RT_{iso}$ is related to the isokinetic temperature (T_{iso}). In agreement with Vyazovkin and Linert[45], a T_{iso} value which is in or close to the experimental temperature range indicates that the kinetic model describes the reactive process accurately.

Figure 6 shows the IKR plot for the third degradation stage of Folnak® samples evaluated by the KAS model-free method in the α range of $0.30 \le \alpha \le 0.80$.

From the IKR plot presented through Equation (13), the isokinetic temperature (T_{iso}) can be found. The value of T_{iso} was found to be 149.8°C. The calculated value of T_{iso} lies in the experimental temperature range for considered third degradation stage of Folnak® sample. This result indicates that if the isokinetic temperature lies in the experimental temperature range, attesting real physical significance, then we can find the appropriate mathematical form of the function of the kinetic model, which best describes the investigated degradation stage.

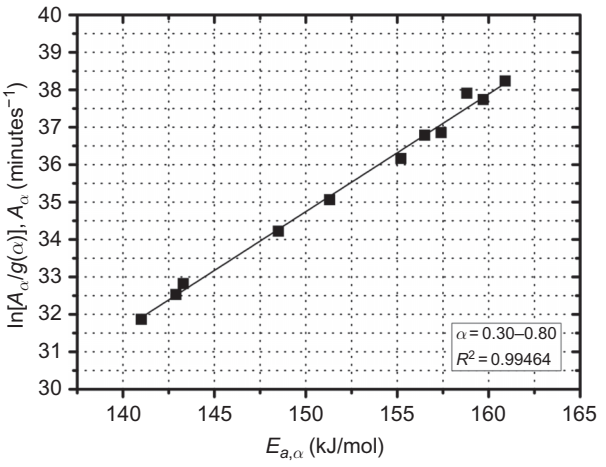

Figure 6. The IKR plot obtained by the Kissinger–Akahira–Sunose isoconversional (model-free) method, for the third degradation stage of the Folnak® sample, in the conversion (α) range of $0.30 \le \alpha \le 0.80$.

The evaluation of the kinetic model function

If the Folnak® sample is complex, then its degradation process may include parallel, concurrent, or consecutive steps of many elementary reactions[46].

Figure 5 shows that the apparent activation energy manifested a little variation with the extent of conversion in the range of [0.30, 0.80]. So we can approximately consider that the apparent activation energy of the Folnak® samples is a definite value in this phase, when we investigate the kinetic model. The average value of E_a evaluated by KAS isoconversional method in the α range of [0.30, 0.80] was used for the determination of the kinetic model of the third degradation stage of Folnak® samples.

The most reliable kinetic model can be determined by comparing the $y(\alpha)$ and $z(\alpha)$ functions, according to Equations (7) and (10). The normalized $y(\alpha)$ and $z(\alpha)$ functions for the third degradation stage of Folnak® sample are presented in Figures 7 and 8. In both cases, the $y(\alpha)$ functions at the different heating rates are concave (Figure 7) and the maximums of $z(\alpha)$ functions are $\alpha_p^\infty < 0.633$ (Figure 8).

It can be seen from Figures 7 and 8 that the maxima of $y(\alpha)$ functions are situated at α_m = 0, whereas the maxima of $z(\alpha)$ functions fall in the range of $0.454 \le \alpha_p^\infty \le 0.521$. The condition of $\alpha_m < \alpha_p^\infty$ and $\alpha_p^\infty < 0.633$[47] should be an indication of the ROn ($n > 1$)

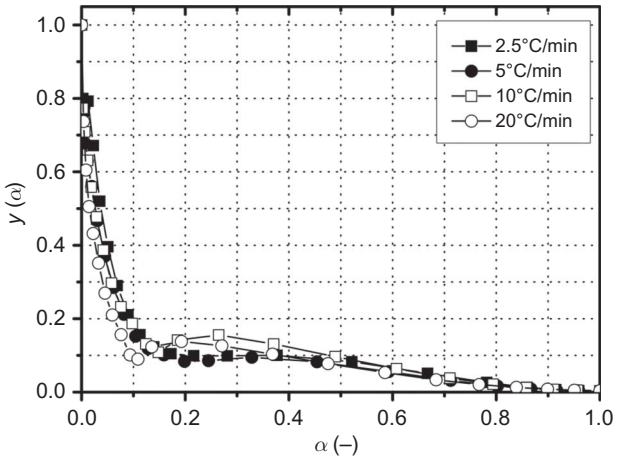

Figure 7. Experimental $y(\alpha)$ function versus α for the third degradation stage of the Folnak® samples at different heating rates (2.5°C/min, 5°C/min, 10°C/min, and 20°C/min).

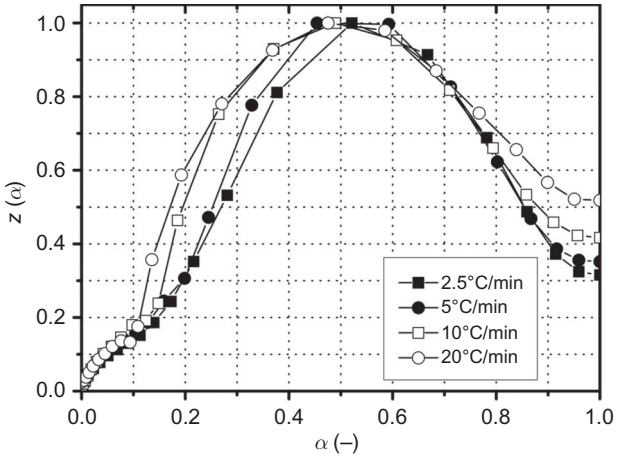

Figure 8. Experimental $z(\alpha)$ function versus α for the third degradation stage of the Folnak® samples at different heating rates (2.5°C/min, 5°C/min, 10°C/min, and 20°C/min).

kinetic model. The most probable kinetic model for the third degradation stage of Folnak® sample is, therefore, the reaction order kinetic model with $n > 1$.

If the kinetic model is known, the equation for nonisothermal $\alpha(T)$ curve can be obtained from Equation (8). For the ROn kinetic model, it can be written in the following form:

$$\alpha(T) = 1 - \left[1 - T\left(\frac{\pi(x)}{\beta}\right)(1-n)A\exp(-x)\right]^{\frac{1}{(1-n)}}. \qquad (14)$$

The temperature dependence of the reduced apparent activation energy ($x = E_a/RT$) can easily be calculated for the average value of the apparent activation energy obtained by the isoconversional method (see above). The values of parameters n and A can be obtained by the nonlinear regression method[48,49] using the experimental data. In this study, the Levenberg–Marquardt method has been used for the calculation of the parameter values. The Levenberg–Marquardt method is a nonlinear regression method. More detailed information about this method can be found in the literature[50]. For performing the Levenberg–Marquardt method, either general purposed mathematical software or a computer program developed in any programming language is used. In this article, the Mathcad® computational software has been used for performing the optimization procedure.

The average values of the parameters n and ln A obtained for third degradation stage of Folnak® sample are shown in Table 2. It can be seen from Table 2 that the values of reaction order (n) fall in the range of $1.59 \leq n \leq 2.21$. The highest value of n was observed at the heating rate of 5°C/min.

The validity of calculated reaction orders for the third degradation stage of Folnak® sample using the nonlinear regression method can be checked directly from the symmetrical index of a DTG peak based on the Kissinger technique[51] by the following equation:

$$n = 1.88\frac{\left|\mathrm{d}^2\alpha/\mathrm{d}t^2\right|_L}{\left|\mathrm{d}^2\alpha/\mathrm{d}t^2\right|_R}, \qquad (15)$$

where the indices L and R correspond to the left and right peak ($\mathrm{d}^2\alpha/\mathrm{d}t^2$) values on the second derivative thermogravimetry (DDTG) curve for the degradation process. Figure 9 shows the DDTG curves obtained for the nonisothermal degradation process of Folnak® sample at the different heating rates. At the same figure, all degradation steps are designated as steps I, II, III, IV, and V.

Using Equation (15), the values of reaction order (n) calculated for the third degradation step of Folnak® sample at the heating rates of 2.5°C/min, 5°C/min, 10°C/min, and 20°C/min are the following: n = 1.60,

Table 2. The kinetic parameters obtained by the nonlinear regression of nonisothermal data using Equation (14) and the constant value of the apparent activation energy (152.3 kJ/mol) for the third degradation stage of Folnak® sample.

	3rd Folnak® degradation stage		
β (°C/min)	n	ln$A$	Residual sum of squares (RSS)
2.5	1.59	35.31	0.00360
5	2.21	35.61	0.00397
10	1.85	35.53	0.00325
20	1.98	35.58	0.00276

Values of the RSS at the corresponding heating rates are also presented in the same table.

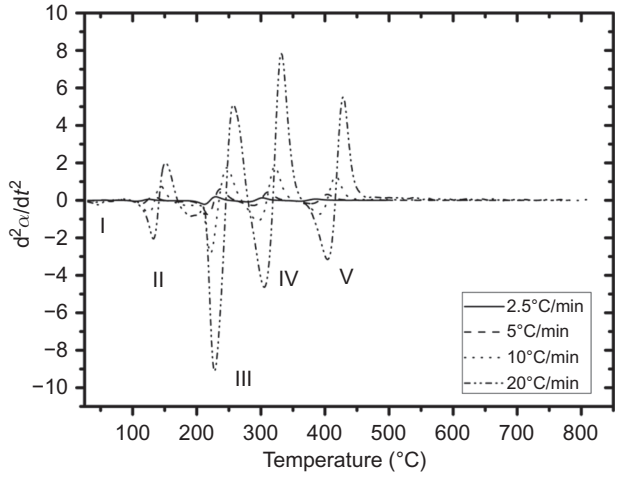

Figure 9. The second DDTG curves for the degradation process of the Folnak® samples at different heating rates (β = 2.5°C/min, 5°C/min, 10°C/min, and 20 °C/min). The corresponding degradation stages are designated as stages I, II, III, IV, and V.

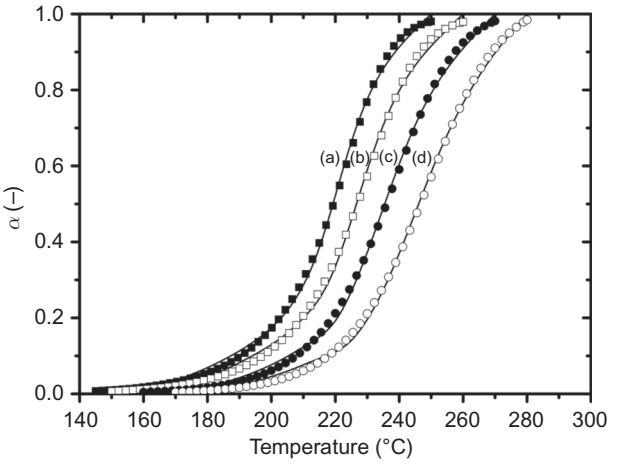

Figure 10. The nonisothermal conversion curves for the decomposition process of the folic acid measured at the different heating rates: (a) (■) calculated $\alpha(T)$ curve at 2.5°C/min; (b) (□) calculated $\alpha(T)$ curve at 5°C/min; (c) (●) calculated $\alpha(T)$ curve at 10°C/min; (d) (○) calculated $\alpha(T)$ curve at 20°C/min; full lines represent the experimental conversion curves at the different heating rates. All symbol curves were calculated using Equation (14) for the kinetic parameters shown in Table 2.

2.24, 1.88, and 1.97, respectively. There is quite good agreement between the values of n calculated by the nonlinear regression method (Table 2) and the values of n evaluated by the graphical method using Equation (15).

It can be observed from Table 2 that the reaction order in this stage was changed from 1.59 to 2.21 according to the heating rate of the system. The observed variation of the reaction order was suggested because of the complex reaction pathways of the folic acid degradation. The pathways were composed with a series of reactions, probably the series of competing reactions, and the contribution of each pathway for the total degradation reaction was affected when the heating rate of the system was changed. Therefore, the reaction order was varied with the heating rate (Table 2).

Figure 10 shows the comparison of experimental data plots (full lines) and calculated $\alpha(T)$ plots (point symbols) for the third degradation stage of Folnak® sample. The $\alpha(T)$ curves were calculated using Equation (14) for the kinetic parameters shown in Table 2. There is excellent agreement between the experimental data and the corresponding prediction of the ROn model.

From these results we can conclude that the decomposition mechanism of folic acid cannot be explained by the simple reaction order model (n = 1) but with the complex reaction mechanism, which include the higher reaction orders (n > 1), with average value of n = 1.91.

In this work, we have applied the so-called isothermal predictions, which means that the nonisothermal kinetic parameters can be used to simulate the variation of the extent of conversion (α) versus time (t) for a given (constant) temperature (T_{iso}) without the knowledge of the reaction model. The isothermal predictions of the third degradation stage of Folnak® sample, at four different temperatures (T_{iso} = 180°C, 200°C, 220°C, and 260°C), using the kinetic parameters evaluated for β = 10°C/min are presented in Figure 11.

The shapes of the isothermal conversion curves at lower temperatures (180–200°C) were similar, whereas they became more complex (the conversion curve at 220°C begins to deviate at lower values of α) with further temperature increase because of complex behavior of folic acid decomposition, especially after 220°C. After this temperature, the decomposition process probably proceeds through the overlapping mechanism, which contributes to the additional complexity of the investigated process. These results are in good correlation with nonisothermal experimental TG–DTA curves.

Conclusions

Thermal stability and nonisothermal kinetics of Folnak® degradation process were investigated by TG–DTG–DTA techniques in the temperature range from an ambient one up to 810°C. It was concluded that the degradation of Folnak® powder sample proceeds through the five stages (designated as stages I, II, III, IV, and V). These stages include the dehydration (I), the melting process of excipients (II), decomposition processes of folic acid (III), corn starch (IV), and saccharose (V). Also, it was observed that the presence of CO_2 (which evolved as a product of carbonate decomposition) at high temperature reacts with residual char to form CO

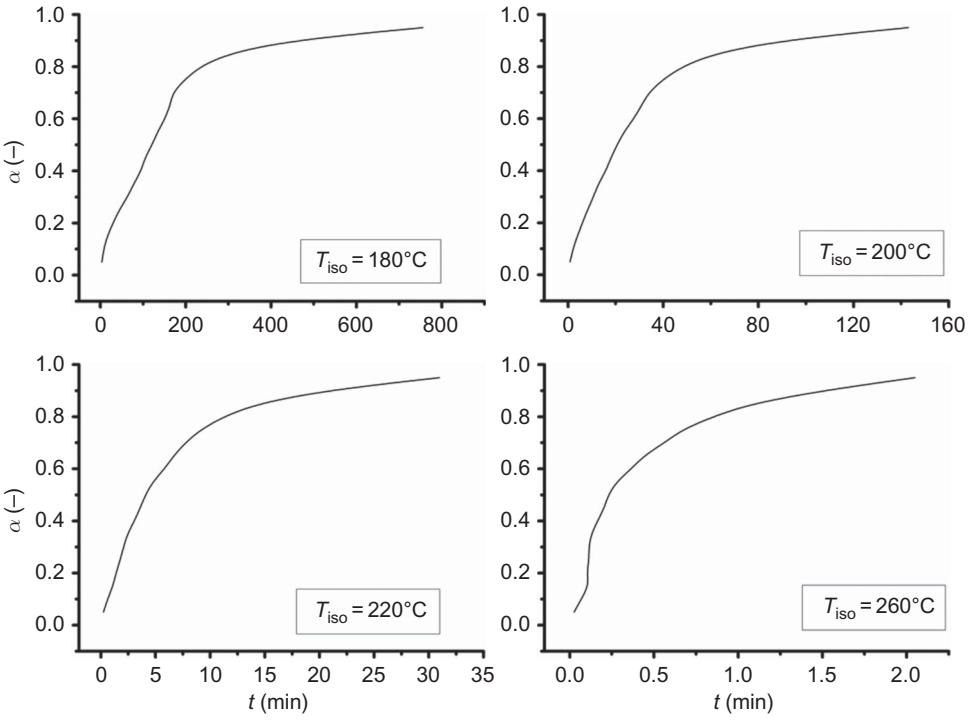

Figure 11. Predictions of the isothermal decomposition kinetics of the folic acid at the different temperatures, T_{iso} = 180°C, 200°C, 220°C, and 260°C, using the kinetic parameters evaluated for the heating rate of β = 10°C/min.

causing additional mass loss, which is included in the final Folnak® degradation stage. In the case of Folnak® degradation, some kind of solid–solid and/or solid–gas interaction was presented.

It was concluded that the main degradation stage of Folnak® sample represents the decomposition reaction of folic acid. The apparent activation energy of the folic acid decomposition under Folnak® degradation process was calculated by the KAS and Ozawa methods. The results show that the apparent activation energy is not a constant throughout the considered decomposition process. But in the conversion range of $0.30 \leq \alpha \leq 0.80$, the apparent activation energy changes slightly, for which the average value is 152.3 kJ/mol, calculated by the KAS method.

By applying the two special functions [$y(\alpha)$ and $z(\alpha)$ functions], the kinetic model was determined for the third degradation stage. It was concluded that the reaction order kinetic model (ROn with $n > 1$) represents the most probable kinetic model for the kinetic description of the third degradation stage. Using the nonlinear regression method, the kinetic parameters (n and ln A) for the third degradation stage of Folnak® sample were determined. It was found that there is good agreement between the values of n calculated by the nonlinear regression method and by the graphical method.

The isothermal predictions of the third degradation stage of Folnak® sample, at four different temperatures (T_{iso} = 180°C, 200°C, 220°C, and 260°C), were presented in this article. It was concluded that the shapes of the isothermal conversion curves at lower temperatures (180–200°C) were similar, whereas they became more complex with further temperature increase because of complex behavior of folic acid decomposition, especially after 220°C. It is assumed that after this temperature, the decomposition process probably proceeds through the overlapping mechanism, which contributes to additional complexity of the investigated process. Finally, the isothermal predictions are in good correlation with nonisothermal TG–DTA measurements.

Declaration of interest

This study was partially supported by the Ministry of Science and Development of Serbia, under the following Projects 142025 and 142047 (Slavko Mentus). The (revised) manuscript entitled 'Thermal Stability and Nonisothermal Kinetics of Folnak® Degradation Process' is not concurrently under the consideration for publication in another journal and the authors do not have any potential conflict of interest. The authors report no declaration of interest.

References

1. Hoffbrand AV, Weir DG. (2001). The history of folic acid. Br J Haematol, 113:579–89.
2. Lam YF, Kotowycz G. (1972). Self association of folic acid in aqueous solution by proton magnetic resonance. Can J Chem, 50:2357–63.
3. Akhtar JM, Khan AM, Ahmad I. (1999). Photodegradation of folic acid in aqueous solution. J Pharm Biomed Anal, 19:269–75.
4. Grzelak A, Rychlik B, Bartosz G. (2001). Light-dependent generation of reactive oxygen species in cell culture media. Free Radic Biol Med, 30:1418–25.
5. Ebisch IMW, Thomas CMG, Peters WHM, Braat DDM, Steegers-Theunissen RPM. (2007). The importance of folate, zinc and antioxidants in the pathogenesis and prevention of subfertility. Hum Reprod Update, 13:163–74.
6. Samuel CE, Rabinowitz JC. (1974). Initiation of protein synthesis by folate-sufficient and folate-deficient Streptococcus faecalis R. J Biol Chem, 249:1198–206.
7. Helms RA, Herfindal ET, Quan DJ, Gourley DR. (2006). Textbook of therapeutics: Drug and disease management. 8th ed. Philadelphia, PA: Lippincott Williams & Wilkins, Wolters Kluwer Health, 75–95.
8. Gomber S, Kela K, Dhingra N. (1998). Clinico-hematological profile of megaloblastic anemia. Indian Pediatr, 35:55–8.
9. Gomber S, Dewan P, Dua T. (2004). Homocystinuria: A rare cause of megaloblastic anemia. Indian Pediatr, 41:941–3.
10. Roy S, Riga AT, Alexander KS. (2002). Experimental design aids the development of a differential scanning calorimetry standard test procedure for pharmaceuticals. Thermochimica Acta, 392–393:399–404.
11. Waterman KC, Adami RC. (2005). Accelerated aging: Prediction of chemical stability of pharmaceuticals. Int J Pharm, 293:101–125.
12. Vyazovkin S. (2006). Thermal analysis. Anal Chem, 78:3875–86.
13. Cides LCS, Araújo AAS, Santos-Filho M, Matos JR. (2006). Thermal behaviour, compatibility study and decomposition kinetics of glimepiride under isothermal and non-isothermal conditions. J Therm Anal Calorim, 84:441–5.
14. Araújo AS, Storpirtis S, Mercuri LP, Carvalho FMS, Santos Filho M, Matos JR. (2003). Thermal analysis of the antiretroviral zidovuine (AZT) and evaluation of the compatibility with excipients used in solid dosage forms. Int J Pharm, 260:303–14.
15. Rodante F, Vecchio S, Tomassetti M. (2002). Kinetic analysis of thermal decomposition for penicillin sodium salts: Model-fitting and model-free methods. J Pharm Biomed Anal, 29:1031–43.
16. Hatakeyama T, Quinn FX. (1994). Thermal analysis: Fundamentals and applications to polymer science. 2nd ed. Chichester, UK: John Wiley & Sons, 158.
17. Tønnesen HH, Moore DE. (1991). Photochemical stability of biologically active compounds. III. Mefloquine as a photosensitizer. Int J Pharm, 70: 95–101.
18. Brown ME, Dollimore D, Galwey AK. (1980). Reactions in solid state. In: Bamford CH, Tipper CFH, eds. Comprehensive chemical kinetics, vol. 22. Amsterdam: Elsevier, 22–3.
19. Senum GI, Yang RT. (1977). Rational approximations of the integral of the Arrhenius equation. J Therm Anal Calorim, 11:445–7.
20. Vyazovkin S, Wight CA. (1999). Model-free and model-fitting approaches to kinetic analysis of isothermal and nonisothermal data. Thermochimica Acta, 340–341, 53–68.
21. Vyazovkin S. (2000). Computational aspects of kinetic analysis: Part C. The ICTAC kinetics project—the light at the end of the tunnel? Thermochimica Acta, 355:155–63.
22. Khawam A, Flanagan DR. (2006). Basics and applications of solid-state kinetics: A pharmaceutical perspective. J Pharm Sci, 95:472–98.
23. Kissinger HE. (1957). Reaction kinetics in differential thermal analysis. Anal Chem, 29:1702–6.
24. Akahira T, Sunose T. (1971). Joint convention of four electrical institutes. Res Rep Chiba Inst Technol, 16:22–31.
25. Ozawa T. (1965). A new method of analyzing thermogravimetric data. Bull Chem Soc Jpn, 38:1881–6.
26. Friedman HL. (1964). Kinetics of thermal degradation of char-forming plastics from thermogravimetry: Application to a phenolic plastic. J Polym Sci C, 6:183–95.
27. Dickinson CF, Heal GR. (2009). A review of the ICTAC kinetics project, 2000 Part 2. Non-isothermal results. Thermochimica Acta, 494:15–25.
28. Coats AW, Redfern JP. (1964). Kinetic parameters from thermogravimetric data. Nature, 201:68–9.
29. Doyle CD. (1962). Estimating isothermal life from thermogravimetric data. J Appl Polym Sci, 6:639–42.
30. Málek J. (1992). The kinetic analysis of non-isothermal data. Thermochimica Acta, 200:257–69.
31. Criado JM, Málek J, Ortega A. (1989). Applicability of the master plots in kinetic analysis of non-isothermal data. Thermochimica Acta, 147:377–85.
32. Málek J. (1989). A computer program for kinetic analysis of non-isothermal thermo-analytical data. Thermochimica Acta, 138:337–46.
33. Liu X, Yu L, Liu H, Chen L, Li L. (2008). In situ thermal decomposition of starch with constant moisture in a sealed system. Polym Degrad Stab, 93:260–2.
34. Beninca C, Demiate IM, Lacerda LG, Carvalho Filho MAS, Ionashiro M, Schnitzler E. (2008). Thermal behavior of corn starch granules modified by acid treatment at 30°C and 50°C. Ecl Quím São Paulo, 33:13–8.
35. Suñol JJ, Farjas J, Berlanga R, Saurina J. (2000). Thermal analysis of a polyethylene glycol (PEG 4000): T-CR-T diagram construction. J Therm Anal Calorim, 61:711–8.
36. Bartsch SE, Griesser UJ. (2004). Physicochemical properties of the binary system glibenclamide and polyethylene glycol 4000. J Therm Anal Calorim, 77:555–69.
37. Zobel HF. (1984). Gelatinization of starch and mechanical properties of starch pastes. In: Whistler RL, Bemiller JN, Paschall EF, eds. Starch: Chemistry and technology. Orlando, FL: Academic Press, Inc., 285–309.
38. Mura P, Faucci MT, Manderioli A, Bramanti G, Ceccarelli L. (1998). Compatibility study between ibuproxam and pharmaceutical excipients using differential scanning calorimetry, hot-stage microscopy and scanning electron microscopy. J Pharm Biomed Anal, 18:151–63.
39. Dollimore D, Evans TA, Lee YF, Pee GP, Wilburn FW. (1992). The significance of the onset and final temperatures in the kinetic analysis of TG curves. Thermochimica Acta, 196:255–65.
40. Wright SF, Dollimore D, Dunn JG, Alexander K. (2004). Determination of the vapor pressure curves of adipic acid and triethanolamine using thermogravimetric analysis. Thermochimica Acta, 421:25–30.
41. Guggenheim S, Koster van Groos AF. (2001). Baseline studies of the clay minerals society source clays: Thermal analysis. Clays Clay Miner, 49:433–43.
42. Vora A, Riga A, Dollimore D, Alexander KS. (2002). Thermal stability of folic acid. Thermochimica Acta, 392–393, 209–20.
43. Kim DS, Soderquist CZ, Icenhower JP, McGrail BP, Scheele RD, McNamara BK, et al. (2005). Tc reductant chemistry and crucible melting studies with simulated Hanford low-activity waste. Prepared for the U.S. Department of Energy Under Contract DE-AC05-76RL01830. Richland, WA: Pacific Northwest National Laboratory, 44–7.
44. Yamamura S, Gotoh H, Sakamoto Y, Momose Y. (2000). Physicochemical properties of amorphous precipitates of cimetidine-indomethacin binary system. Eur J Pharm Biopharm, 49:259–265.
45. Vyazovkin S, Linert W. (1995). False isokinetic relationships found in the nonisothermal decomposition of solids. Chem Phys, 193:109–18.
46. Rodante F, Vecchio S, Materazzi S, Vasca E. (2003). Kinetic and thermodynamic study of the $Na_4(UO_2)_2(OH)_4(C_2O_4)_2$ complex. Int J Chem Kinet, 35:661–9.

47. Montserrat S, Málek J, Colomer P. (1998). Thermal degradation kinetics of epoxy-anhydride resins: I. Influence of a silica filler. Thermochimica Acta 1998, 313:83–95.
48. Anderson HL, Kemmler A, Strey R. (1996). Comparison of different non-linear evaluation methods in thermal analysis. Thermochimica Acta, 271:23–9.
49. Opfermann J. (2000). Kinetic analysis using multivariate non-linear regression. I. Basic concepts. J Therm Anal Calorim, 60:641–58.
50. Chong EKP, Zak SH. (2001). An introduction to optimization. New York: John Wiley and Sons, Inc.
51. Huang MR, Li XG. (1998). Thermal degradation of cellulose and cellulose esters. J Appl Polym Sci, 68:293–304.